Cell Metabolism
Article

The Pro12Ala PPARγ2 Variant Determines Metabolism at the Gene-Environment Interface

Sami Heikkinen,[1,2] Carmen Argmann,[1] Jérôme N. Feige,[1] Hana Koutnikova,[1,3] Marie-France Champy,[3] Nassim Dali-Youcef,[4] Eric E. Schadt,[5] Markku Laakso,[6] and Johan Auwerx[1,3,4,7,*]
[1]Institut de Génétique et de Biologie Moléculaire et Cellulaire, CNRS/INSERM/Université Louis Pasteur, 67404 Illkirch, France
[2]A.I.Virtanen Institute for Molecular Sciences, University of Kuopio, 70211 Kuopio, Finland
[3]Institut Clinique de la Souris, 67404 Illkirch, France
[4]Hopitaux Universitaires de Strasbourg, Laboratoire de Biochimie Générale et Spécialisée, 67000 Strasbourg, France
[5]Rosetta Inpharmatics LLC, a wholly owned subsidiary of Merck & Co., Inc., Seattle, WA 98109, USA
[6]Department of Medicine, University of Kuopio, 70211 Kuopio, Finland
[7]Ecole Polytechnique Fédérale de Lausanne, 1015 Lausanne, Switzerland
*Correspondence: admin.auwerx@epfl.ch
DOI 10.1016/j.cmet.2008.11.007

SUMMARY

The metabolic impact of the common peroxisome proliferator-activated receptor gamma isoform 2 (PPARγ2) variant Pro12Ala in human populations has been widely debated. We demonstrate, using a Pro12Ala knockin model, that on chow diet, Ala/Ala mice are leaner, have improved insulin sensitivity and plasma lipid profiles, and have longer lifespans. Gene-environment interactions played a key role as high-fat feeding eliminated the beneficial effects of the Pro12Ala variant on adiposity, plasma lipids, and insulin sensitivity. The underlying molecular mechanisms involve changes in cofactor interaction and adiponectin signaling. Altogether, our results establish the Pro12Ala variant of Pparγ2 as an important modulator in metabolic control that strongly depends on the metabolic context.

INTRODUCTION

Peroxisome proliferator-activated receptor gamma (PPARγ), and especially the PPARγ2 isoform, is a ligand-dependent nuclear receptor highly expressed in adipose tissue, where it coordinates a thrifty phenotype by promoting adipocyte differentiation and triglyceride storage (Auwerx, 1999; Fajas et al., 1997; Lehrke and Lazar, 2005; Tontonoz et al., 1994b). The metabolic functions of PPARγ also include the coordination of glucose homeostasis and insulin sensitivity (Knouff and Auwerx, 2004). Consequently, synthetic PPARγ agonists such as the thiazolidinediones (TZDs) have proven valuable in the pharmacological management of type 2 diabetes (T2DM) (Lehmann et al., 1995).

The common Pro12Ala variant of PPARγ2 (Ala frequency 920% [Heikkinen et al., 2007]) causes a moderate decrease in its transcriptional activity and adipogenic potential (Deeb et al., 1998; Masugi et al., 2000). We previously associated the Pro12 variant with the risk of T2DM (Deeb et al., 1998). Recent meta-analyses (Florez et al., 2003; Ludovico et al., 2007; Tönjes et al., 2006) and genome-wide association studies (GWAS) (Saxena et al., 2007; Scott et al., 2007; Sladek et al., 2007; Steinthorsdottir et al., 2007; Zeggini et al., 2007) have confirmed our original findings. The Ala12 allele has also been associated with reduced weight gain and improved insulin sensitivity, particularly in lean subjects (Altshuler et al., 2000; Deeb et al., 1998; Ek et al., 1999). However, these observations have been challenged, especially in obese subjects where the Ala allele has been associated with increased weight gain (Ek et al., 1999). Thus, the Pro12Ala genotype appears to be sensitive to environmental influence, such that the Ala allele is beneficial in lean subjects but could be detrimental when coexisting with obesity.

Genetic association studies are valuable to identify potential disease genes. Ultimately, however, a mouse model system is needed to understand the mechanistic impact of such genes and their variants. We have generated a knockin mouse model for the PPARγ2 Pro12Ala variant to understand the fundamental physiological and molecular roles of PPARγ2 and its Pro12Ala variant. Our results strengthen the view that the Pro/Pro of *PPARG2* is a risk genotype that adversely affects glucose homeostasis and lifespan. Furthermore, the protective role of the Ala/Ala genotype depends on the dietary context, suggesting that the metabolic impact of this mutation is highly dependent on gene-environment interactions.

RESULTS

Generation of the Pparγ2 Pro12Ala Knockin Mouse

In order to analyze the consequences of the Pparγ2 Pro12Ala mutation in a well-defined and controllable genetic background, this mutation was introduced into the mouse genome (Figure 1A). Pparγ2 Pro12Ala mice bred normally and transmitted the variant allele to their offspring at the expected Mendelian ratios (Figure 1B). Sequencing confirmed the presence of the CCA → GCA mutation (Pro → Ala) at codon 12 of *Pparg2* exon B without additional changes in the coding sequence (data not shown). Using an allele-specific qRT-PCR strategy, both Pro and Ala alleles were confirmed to express *Pparg2* mRNA at equal levels in Pro/Ala adipose tissue (Table S1), proving a lack of interference by the short cloning remnants surrounding exon B in the Ala allele. The expression of *Pparg1* tended to be increased in epididymal white adipose tissue

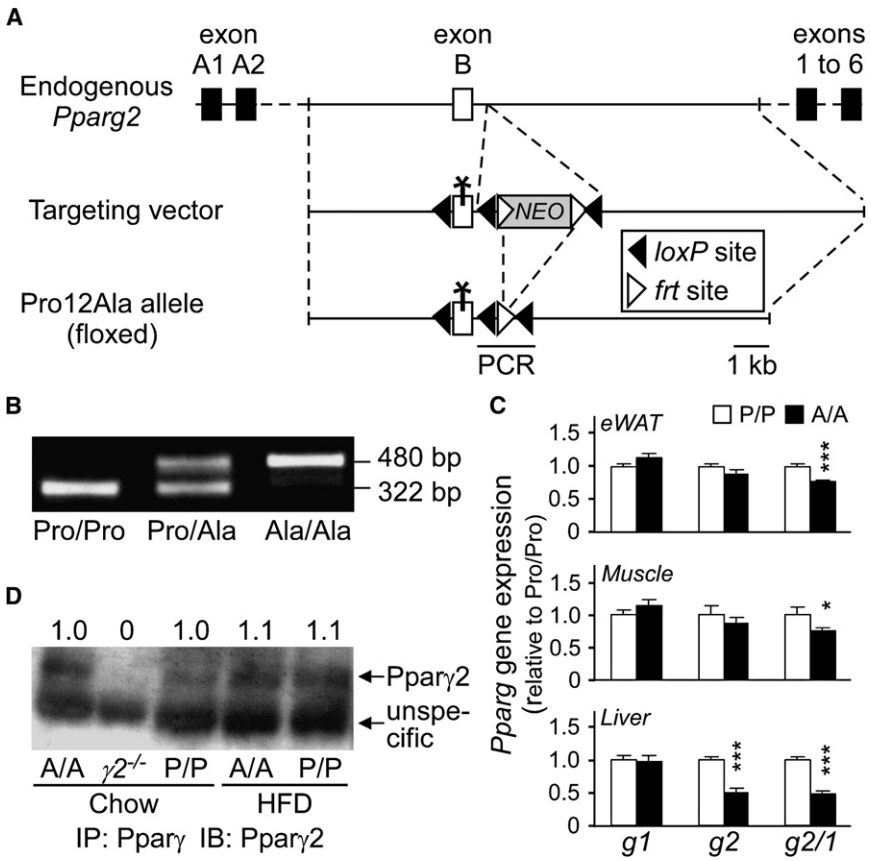

Figure 1. Floxed Pparγ2 Pro12Ala Knockin Construct and the Validation of the Resulting Mouse Model

(A) Construct design and recombination scheme. Filled and open arrowheads indicate *loxP* and *frt* sites, respectively (not to scale). Asterisk indicates the location of Pro12Ala mutation in exon B. The target region for the genotyping PCR is indicated.

(B) PCR genotyping over the *frt* and *loxP* sites, showing products from wild-type (322 bp) and knockin (480 bp) alleles from wild-type (*Pro/Pro*), heterozygous (*Pro/Ala*), and knockin (*Ala/Ala*) mice.

(C) *Pparg1* (*g1*) and *Pparg2* (*g2*) mRNA expression and their ratio (*g2/1*) in eWAT, gastrocnemius muscle, and liver of 8-week-old, chow-fed mice by qRT-PCR, normalized to *Ppib* expression for eWAT and for *Ppib* and *18S* rRNA expression for muscle and liver (n = 9 Pro/Pro and 13 Ala/Ala mice). Data are presented as means ± SEM *, $p < 0.05$; ***, $p < 0.001$ between the groups.

(D) Pparγ2 protein content in Ala/Ala eWAT on both chow and HFD, with WAT from Pparγ2 knockout mice ($\gamma 2^{-/-}$) as control. Immunoprecipitated (IP) total Pparγ protein fraction was immunoblotted (IB) using a Pparγ2-specific antibody. Densitometric quantitation of the Pparγ2 protein amounts is shown above the blot.

(eWAT) of Ala/Ala mice (n = 9 for Pro/Pro and 13 for Ala/Ala, +14.0%, p = 0.128), and a concomitant tendency for a decrease in *Pparg2* expression (−10.8%, p = 0.187) resulted in a significant decrease in the *Pparg2/1* mRNA ratio (−22.0%, p = 0.00014), which could influence the metabolic actions of *PPARG* (Hotta et al., 1998; Vidal-Puig et al., 1997) (Figure 1C, upper panel). Similar changes were seen also in gastrocnemius muscle (Figure 1C, middle panel). In the liver, where *Pparg2* is much less expressed than in WAT, the changes in *Pparg2* expression and *Pparg2/1* ratio were even more pronounced (−49.9%, $p = 1.9 \times 10^{-5}$; and −51.3%, $p = 4.9 \times 10^{-7}$; respectively) (Figure 1C, lower panel). In line with the gene expression results, the Pro12Ala mutation did not noticeably alter Pparγ2 protein levels in WAT (Figure 1D).

Pparγ2 Ala12 Improves Insulin Sensitivity and Lipid Profiles on Chow Diet

The metabolic phenotyping of Pparγ2 Pro12Ala knockin mice in well-controlled environmental and genetic settings offers an excellent means to uncover the full extent of physiological consequences of the variant. On a chow diet, Ala/Ala mice gained less weight than Pro/Pro mice (Figure 2A) despite equal food intake (data not shown). Accurate body length measurement by DEXA scan allowed reliable calculation of the BMI (Figure 2A, inset), which was strikingly lower in 9-month-old Ala/Ala mice (31.2 ± 0.5 versus 35.5 ± 0.7 g/cm^2, p = 0.0006). DEXA scan also revealed that not only fat mass (−35%) but also lean body mass (−8%) was reduced in Ala/Ala mice (Figure 2B). Histological analysis of eWAT as well as BAT suggested that adipocyte size was not affected in Ala/Ala mice (Figure 2C), although the size of individual fat pads at 12 months of age was smaller in Ala/Ala than in Pro/Pro mice (for eWAT, −59%, p = 0.0202; subcutaneous WAT, −61%, p = 0.0018; retroperitoneal WAT, −66%, p = 0.0064; and a tendency for interscapular BAT, −30%, p = 0.0726) (Figure 2D). Fittingly, cultured Ala/Ala mouse embryonic fibroblasts (MEFs), when challenged by an adipogenic differentiation cocktail, contained less cells stained with Oil red O (Figure 2E, upper panel) and had 35% lower total triglyceride content (p = 0.0013) (Figure 2E, lower left panel). Furthermore, the expression of direct Pparγ target genes, such as fatty acid binding protein 4 (*Fabp4*, also called *aP2*) and Cd36 antigen (*Cd36*), was reduced in differentiated Ala/Ala cells (Figure 2E, lower right panel).

Both pharmacological and genetic analyses of PPARγ function have suggested that this receptor can affect bone formation through functional alterations in osteoblasts and osteoclasts (Cock et al., 2004; Wan et al., 2007). DEXA scan showed a small but significant increase in both total bone area (+5.7%, p = 0.029) and bone mineral content (BMC) (+8.9%, p = 0.016) in Ala/Ala mice (Figure 2F). However, bone mineral density (BMD) was not altered. Furthermore, the Ala/Ala mice did not have splenomegaly (data not shown).

Biochemical analysis revealed an improved plasma lipid profile in 6- to 8-week-old Ala/Ala homozygotes on chow diet (Figure 3A, upper panel). A small decrease in total cholesterol (Chol) and triglyceride (TG) levels was accompanied by a robust 71% decrease in the Chol content of LDL particles (p = 0.0042),

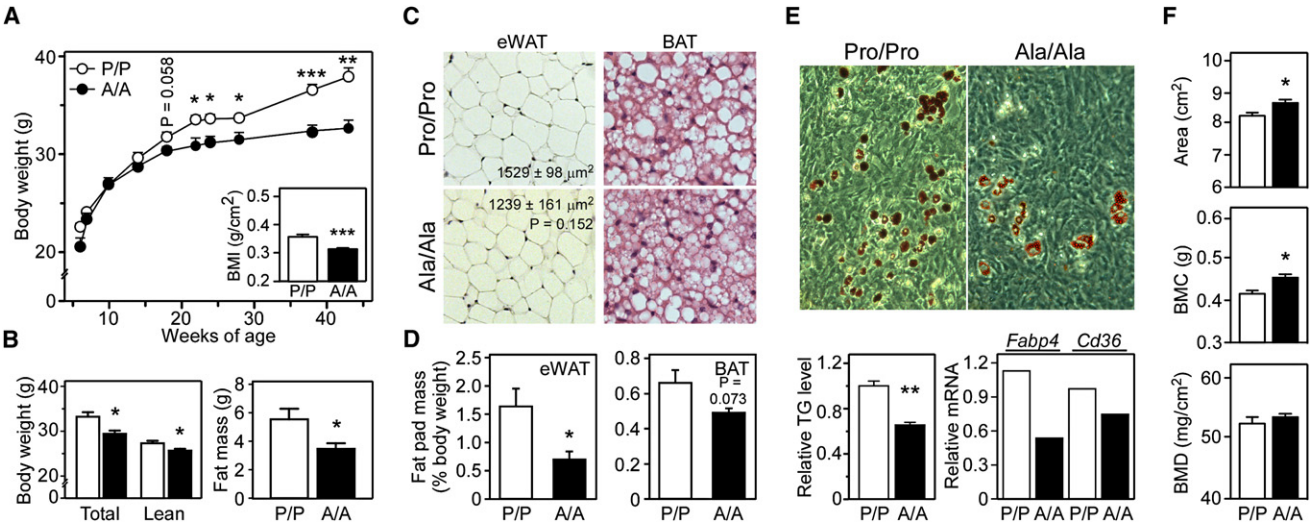

Figure 2. Growth, Body Composition, and Adipocyte Differentiation of Pparγ2 Pro12Ala Knockin Mice on Chow

(A) Body weight development, measured periodically from 6 weeks of age. In the inset, BMI at 37 weeks of age.

(B) Total and lean body weight (left) and body fat mass (right) by DEXA scan at 37 weeks of age.

(C) eWAT (left) and BAT (right) histology as representative hematoxylin-eosin stained sections. Adipocyte sizes are indicated for eWAT of chow-fed mice (n = 4–5 per group).

(D) Fat pad weights for eWAT (left) and BAT (right).

(E) Adipocyte differentiation of MEFs, shown as representative micrographs of cells in culture (top), quantified relative triglyceride content of n = 3 replicate cultures of differentiated cells (lower left), and representative effects on the mRNA expression of Pparγ target genes (*Fabp4* and *Cd36*), normalized to *18S* rRNA expression.

(F) Whole body bone area (top), BMC (middle), and BMD (bottom) by DEXA scan at 37 weeks of age. Data are presented as means ± SEM, and for (A), (B), (D), and (F), n = 5–8 per group. *, $p < 0.05$; **, $p < 0.01$; and ***, $p < 0.001$ between the Pro/Pro (P/P) and Ala/Ala (A/A) groups.

without changes in the Chol content of either VLDL or HDL particles (data not shown). However, none of fasting free fatty acids (FFAs), glucose, insulin, leptin, nor adiponectin levels differed between Pro/Pro and Ala/Ala mice (Figure 3A). A similar metabolite profile also persisted in older animals (data not shown). Of note, both liver weight and the hepatic lipid profile were unchanged between Pro/Pro and Ala/Ala mice (data not shown).

The Ala12 allele associates with a reduced risk of T2DM by meta-analyses and GWAS in humans (Deeb et al., 1998; Florez et al., 2003; Ludovico et al., 2007; Saxena et al., 2007; Scott et al., 2007; Sladek et al., 2007; Steinthorsdottir et al., 2007; Tönjes et al., 2006; Zeggini et al., 2007). Similarly, the Ala/Ala mice had enhanced glucose tolerance in an intraperitoneal glucose tolerance test (IPGTT) (Figure 3B). Moreover, euglycemic-hyperinsulinemic clamp showed a clear improvement in the insulin sensitivity of Ala/Ala mice, as the glucose infusion rate (GIR) to maintain their euglycemia was significantly higher than that of Pro/Pro mice (Figure 3C). This result was confirmed in a separate experiment (top left panel in Figure 3D), where the tissues contributing to the improved insulin sensitivity of Ala/Ala mice were determined. The basal rate of glucose appearance (Ra) or hepatic glucose production (top middle panel in Figure 3D) as well as glucose uptake into liver upon insulin stimulation (lower left panel in Figure 3D) were unaltered between Pro/Pro and Ala/Ala mice, suggesting that differences in liver glucose metabolism do not explain our findings. However, there was a 2-fold increase ($p = 0.0013$) in glucose uptake into Ala/Ala WAT (lower left panel in Figure 3D), suggesting a role for WAT in the improved insulin sensitivity of Ala/Ala mice on chow. The increase in glucose uptake into Ala/Ala muscles did not reach statistical significance (lower panel in Figure 3D), but considering the lack of any difference in the liver and the relatively small overall contribution of WAT to the whole body glucose utilization, contribution from skeletal muscle to the improved GIR and glucose disappearance rate of Ala/Ala mice cannot be completely excluded (top panel in Figure 3D). The observed changes in glucose uptake in Ala/Ala WAT and muscle were not associated, however, with altered basal Glut4 protein or mRNA expression (data not shown). Glucose uptake by the heart and brain were unchanged between Pro/Pro and Ala/Ala mice.

Environmental and especially nutritional factors modulate the phenotypic effects of the Pro12Ala variant in humans (Luan et al., 2001; Memisoglu et al., 2003). To uncover any differences in how Pro/Pro and Ala/Ala mice metabolize lipids versus carbohydrates for energy, we measured their energy expenditure by indirect calorimetry. However, respiratory exchange ratio (RER) did not differ between Pro/Pro and Ala/Ala mice on chow (top panel in Figure 3E). Simultaneous measurement of spontaneous locomotor activity showed that Ala/Ala mice were more active during the onset of the dark period (bottom panel in Figure 3E) and, perhaps consequently, produced more heat and consumed more water, but without altering food intake (Figure S2).

Finally, blood pressure did not differ between Pro/Pro and Ala/Ala mice (99.1 ± 2.5 versus 102 ± 1.4 mmHg, p = NS).

Pparγ2 Ala12 Improves Longevity

The Ala12 variant of Pparγ2 has been suggested to increase longevity in humans (Barbieri et al., 2004). Since the reduction in fat

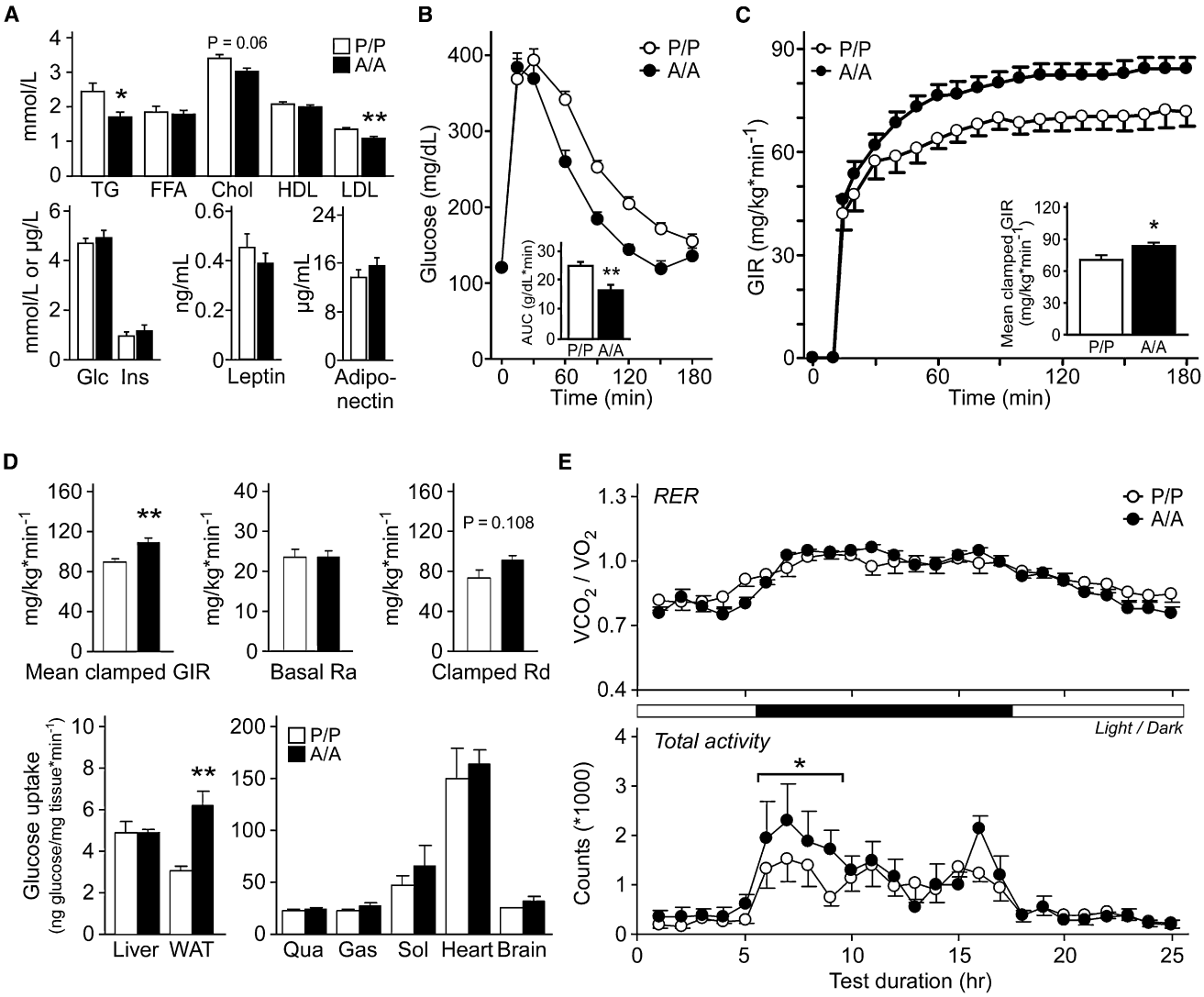

Figure 3. Plasma Metabolite Profile, Insulin Sensitivity, Glucose Utilization, Respiratory Exchange Ratio, and Total Spontaneous Locomotor Activity of Pparγ2 Pro12Ala Mice on Chow

(A) Plasma concentrations for triglycerides (TG), FFAs, total cholesterol (Chol), HDL and LDL cholesterol (upper); and glucose (Glc, mmol/L), insulin (Ins, µg/L), leptin, and adiponectin (lower) (n = 9–16).

(B) Glucose tolerance by IPGTT. The inset shows the area under the glucose curve above baseline (AUC) (n = 6–7).

(C) Insulin sensitivity by euglycemic-hyperinsulinaemic clamp, shown as GIRs (mg/kg*min^{-1}) over the whole test duration, and in the inset, averaged over the clamped period, i.e., the last 60 min (n = 7).

(D) Whole body and tissue-specific glucose utilization by euglycemic-hyperinsulinaemic clamp with radiolabeled glucose and 2-deoxyglucose tracers. The top panel shows, in mg/kg*min^{-1}, GIRs, basal rates of glucose appearance (Ra, i.e., hepatic glucose production), and insulin-stimulated rates of glucose disappearance (Rd) (n = 4–6). The bottom panel shows, in ng glucose/mg tissue*min^{-1}, insulin-stimulated glucose uptake into liver and WAT (left graph) and into quadriceps (Qua), gastrocnemius (Gas) and soleus (Sol) muscles, heart, and brain (right graph).

(E) RER (top) and total spontaneous locomotor activity (bottom) (n = 6–8). Statistically significant differences are shown only for two or more consecutive points. Data are presented as means ± SEM *, $p < 0.05$; **, $p < 0.01$ between the Pro/Pro (P/P) and Ala/Ala (A/A) groups.

mass of Ala/Ala mice was similar to what occurs during caloric restriction and subsequent lifespan extension (Bordone and Guarente, 2005), and in view of the improved metabolic profile, we hypothesized that the variant might have a beneficial effect on lifespan. The Ala/Ala mice indeed lived on average 13% longer on chow than their Pro/Pro littermates (109.6 ± 0.35 versus 123.9 ± 0.97 weeks, p = 0.002) (Figure 4). This result confirms the previous, suggestive results on humans (Barbieri et al., 2004) and demonstrates how the beneficial metabolic effects of the Ala variant project onto the lifelong survival of the organism.

Metabolic Benefits of the Pparg2 Ala12 Allele Are Eliminated upon High-Fat Feeding

The consequences of the Pro12Ala mutation on obesity in human populations (Ek et al., 1999; Masud and Ye, 2003) prompted us to challenge our Pro12Ala knockin mice with high-fat feeding.

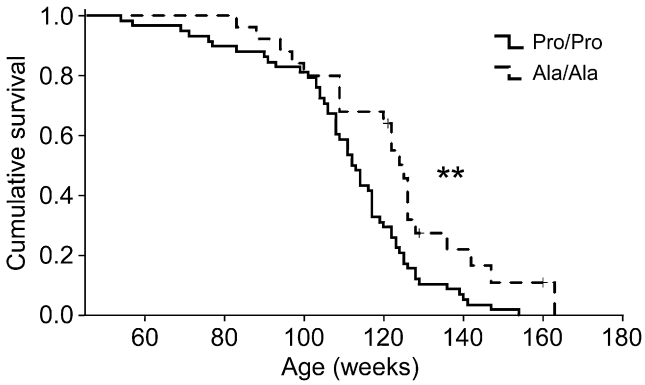

Figure 4. Longevity of Pparγ2 Pro12Ala Mice on Chow
Data are presented as cumulative survival curves. **, $p < 0.01$ between the Pro/Pro (solid line, n = 58) and Ala/Ala (hatched line, n = 25) groups.

Unlike what was observed on chow, Ala/Ala mice on high-fat diet (HFD) appeared somewhat more obese than Pro/Pro mice (Figure 5A). For example, BMI (48.0 ± 3.8 versus 40.1 ± 0.8 g/cm^2, p = 0.125), body weight (at 16 weeks of diet, 39.2 ± 1.98 versus 35.0 ± 0.50 g, p = 0.086), and fat mass (14.6 ± 3.8 versus 10.7 ± 1.5 g, p = 0.359) of Ala/Ala mice tended to exceed that of Pro/Pro mice. Although the differences were not statistically significant, the analysis of chow and HFD data together demonstrated a clear, statistically significant interaction for Pro12Ala genotype and diet on BMI (p = 0.002) and body weight (at 16 weeks of diet, p = 0.017). Fasting plasma glucose or lipid parameters, again in contrast to chow, did not differ between Pro/Pro and Ala/Ala mice on HFD (data not shown). The diet-dependent differences in the Pro12Ala phenotype were also evident at the level of whole body glucose homeostasis, as both IPGTT (Figure 5B) and euglycemic-hyperinsulinemic clamp (Figure 5C) demonstrated the loss of protective effect by the Ala/Ala genotype on HFD. Furthermore, the differences seen on chow in spontaneous activity and heat production were all eliminated on HFD (Figures 5D and S2). Collectively, the greatly increased difference in the adiposity and glucose tolerance of Ala/Ala mice when compared to Pro/Pro mice between the chow and high-fat-fed states (Figure 5E) reveals a diet-dependent metabolic response for the Pro12Ala variant of Pparγ2.

Since Pparγ agonists, like pioglitazone, are widely used insulin sensitizers in the treatment of T2DM, we treated Pparγ2 Pro/Pro and Ala/Ala mice either with HFD or HFD + 0.004% pioglitazone for 5 weeks (Rocchi et al., 2001). The Ala/Ala mice again showed a tendency for increased weight gain (1.10 ± 0.07 versus 0.90 ± 0.07 g/day, p = 0.161), an effect that seemed to be accentuated in Ala/Ala mice on HFD + pioglitazone (1.20 ± 0.09 versus 0.88 ± 0.12 g/day, p = 0.072). However, food intake or insulin sensitivity did not differ between the genotypes (data not shown). Thus, upon caloric excess in mice, Pro12Ala variant appears to modulate pioglitazone effects only mildly.

Pparγ2 Pro12Ala Alters Transcriptional Regulation in Muscle and WAT

To capture the transcriptional effects of the Ala12 mutant isoform of Pparγ2 that potentially underlie the phenotypic changes observed, we performed gene expression microarray analysis of eWAT, gastrocnemius muscle, and liver of 23-week-old males on either chow or 15 weeks HFD (N = 8–10 per group, 112 microarrays in total). Based on the molecular mechanisms through which the Pro12Ala point mutation affects Pparγ action, we expected to find only moderate changes, especially in comparison to the more dramatic changes seen in many *Pparg* gene knockout models (Koutnikova et al., 2003). Indeed, on chow, the expression of only two, six, and one genes, respectively, were altered in Ala/Ala WAT, muscle, and liver, and all by less than 25% (Figure 6A and Table S2). On HFD, more changes were observed in both WAT (46 genes) and muscle (95 genes), although none in the liver, and again the magnitude of change was below 25% (Figure 6A and Table S2).

Considering that the existing evidence points to a reduced transcriptional activity of the Ala12 mutant, and that WAT is the tissue expressing Pparγ2 at the highest level, it is not surprising that in WAT, most genes with changes were downregulated in Ala/Ala mice (76% on HFD, Figure 6A). In contrast, a great majority of genes with altered expression were upregulated in Ala/Ala muscle (~86% in both chow and HFD, Figure 6A). One explanation for this apparent discrepancy could be that in a tissue like muscle, expressing only low levels of Pparγ2, altered signaling from other tissues such as WAT could take precedence.

The most consistent change observed was the upregulation of adiponectin receptor 2 (*Adipor2*) expression in Ala/Ala WAT and muscle on both chow and HFD (Figure 6A and Table S2). Interestingly, adiponectin (*Adipoq*) expression itself was upregulated in Ala/Ala muscle on HFD. *Adipoq* was also upregulated in the muscle of 8-week-old, chow-fed Ala/Ala mice in an independent analysis by qRT-PCR (data not shown). These observations suggest that adiponectin signaling likely plays a role in the phenotypic effects seen in Pparγ2 Pro12Ala mice.

Due to the low number of Pro12Ala-associated changes, we opted to use Gene Set Enrichment Analysis (GSEA) that detects significantly coregulated sets of genes even when the individual genes do not contribute significantly (Mootha et al., 2003; Subramanian et al., 2005). In addition to the gene sets contained in the KEGG and GenMAPP repositories, we also analyzed smaller groups of gene sets for focused subject areas, selected from the Molecular Signatures Database (http://www.broad.mit.edu/gsea/msigdb). GSEA demonstrates a considerable concentration of enrichment in gene sets containing genes upregulated in the muscle of HFD-fed Ala/Ala mice (Figure S3 and Tables S3 and S4), suggesting a role for muscle in the Pro12Ala phenotype. The focused approach provided evidence that such signaling molecules as leptin and other adipocytokines (e.g., adiponectin); mTor, Chrebp, and insulin ('Signaling' subset); and Ppars in general ('Ppar and thiazolidinedione effects' subset) are associated to the loss of protective effects of the Ala allele upon caloric excess (Table S4). In the muscle of high-fat-fed mice, Pro12Ala may also target fatty acid metabolism and genes that become upregulated in obesity ('Metabolism, diabetes, and obesity' subset, Table S4). Surprisingly, however, only G protein-related gene sets had significant enrichment in WAT (Figure S3 and Tables S3 and S4). Together with the observation that nearly all enrichments in the liver were also found in G protein-related gene sets, this suggests a previously poorly described connection between the Pparγ2 Pro12Ala variant and G protein function.

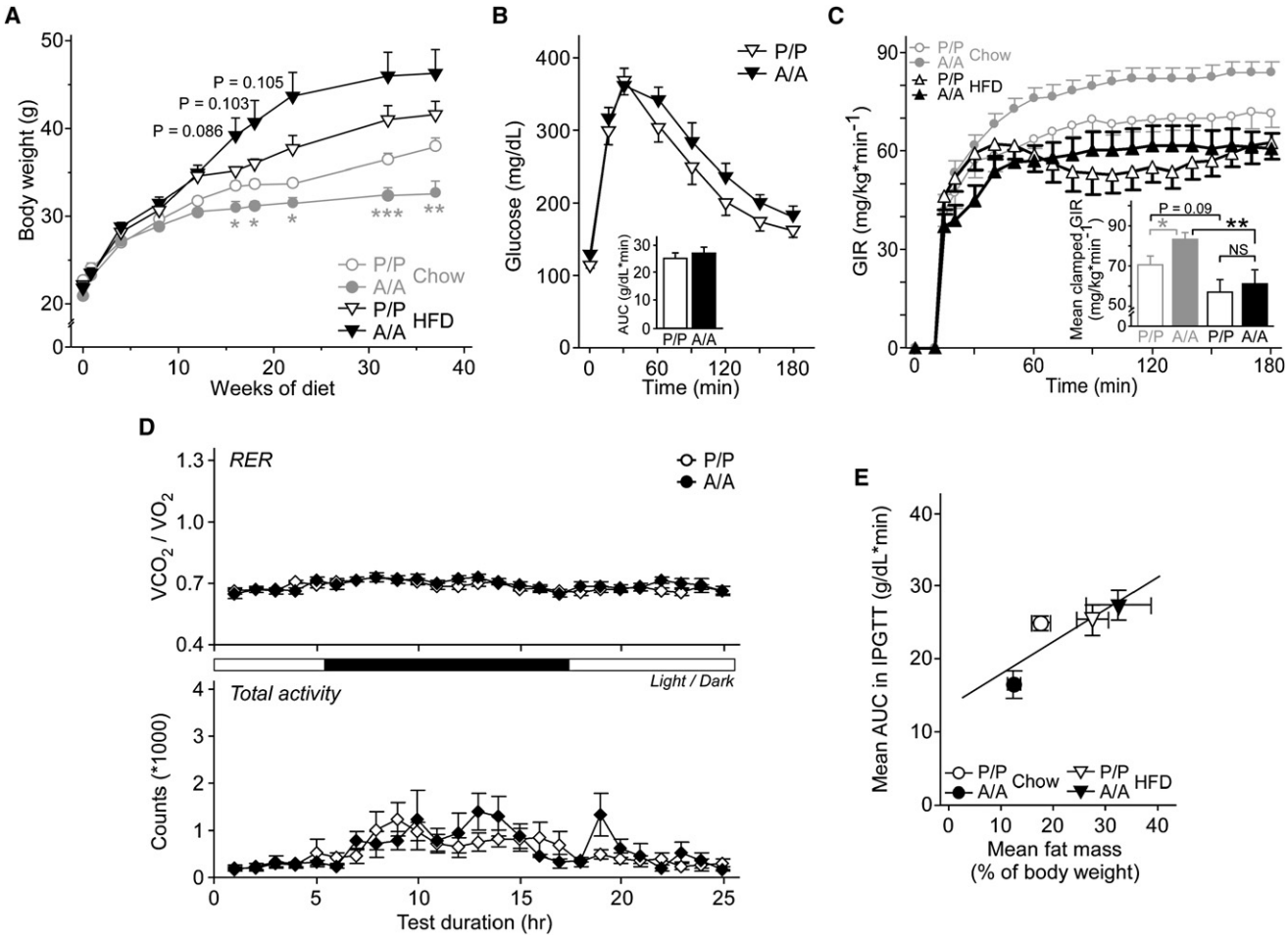

Figure 5. Body Weight Development, Insulin Sensitivity, Respiratory Exchange Ratio, and Spontaneous Locomotor Activity of Pparγ2 Pro12Ala Knockin Mice on High-Fat Diet

(A) Body weight development, measured periodically from 6 weeks of age. The weight curves on chow from Figure 3A are shown for comparison in gray.

(B) Glucose tolerance by IPGTT, conducted after 6 months of high-fat feeding. The inset shows the AUC.

(C) Insulin sensitivity by euglycemic-hyperinsulinaemic clamp, shown as GIRs (mg/kg*min^{-1}) over the whole test duration and, in the inset, averaged over the clamped period, i.e., the last 60 min. The corresponding data on chow from Figure 4C are provided for comparison in gray.

(D) RER (top) and total spontaneous locomotor activity (bottom) (n = 6–8; same mice as in Figure 3E, but after 8 weeks of HFD). Statistically significant differences in two or more consecutive points were not observed.

(E) The diet-dependent effect of the Pro12Ala variant on adiposity and glucose tolerance, visualized by a scatter plot of mean fat mass against the mean AUC for indicated groups. Data are presented as means ± SEM, and n = 4–8 mice per group. *, $p < 0.05$; **, $p < 0.01$; and ***, $p < 0.001$ between the indicated groups of Pro/Pro (P/P) and Ala/Ala (A/A) mice on chow and HFDs.

To further evaluate the implication of adiponectin signaling in the phenotype of the Pro12Ala mutant, we plotted Pearson correlates to both plasma adiponectin levels and *Pparg2* gene expression for all expressed genes to generate 'cocorrelation' graphs (Figure 6B). The ball-like distributions of R^2 values in Pro/Pro WAT on both diets showed that very few genes cocorrelate strongly with adiponectin levels and Pparγ2 expression (top panel in Figure 6B, graphs in blue). However, in Ala/Ala WAT, the shapes of R^2 distributions were elongated on both diets, and moreover, the Ala/Ala distributions were in opposite orientations on chow and HFD (top panel in Figure 6B, graphs in red). The effect of dietary status was limited to Ala/Ala mice also in muscle, where HFD considerably tightened the Ala/Ala cocorrelation distribution (bottom panel in Figure 6B). Collectively, this suggests, at the level of transcriptional regulation, that the Pro12Ala variant sensitizes Pparγ2 to adiponectin signaling, and that the dietary status affects this sensitization.

Altered Cofactor Recruitment by PPARγ2 Pro12Ala Variant

The gene expression changes suggested that the interaction of Pro12 and Ala12 forms of PPARγ2 with other transcriptional coregulators might be altered. We hence used GST pull-down assays to analyze the capacity of Pro12 and Ala12 isoforms of PPARγ2 to interact with a representative set of established PPARγ coregulators in the absence and presence of the PPARγ ligand rosiglitazone (Rosi). Both the ligand-independent and the ligand-dependent interactions with the coactivators MED1 (also

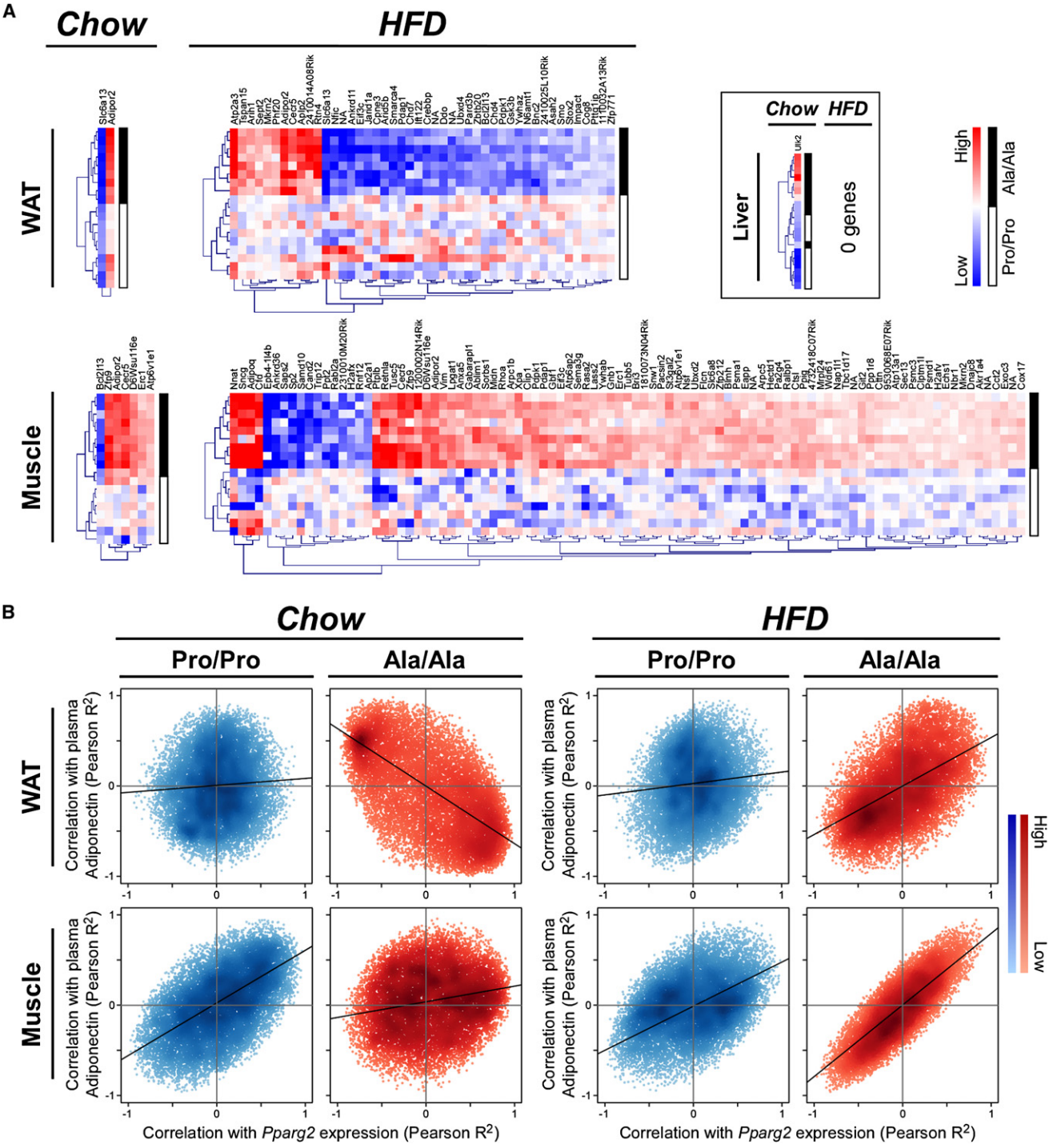

Figure 6. The Impact of Pparγ2 Pro12Ala Variant on Gene Expression Patterns

(A) Hierarchical clustering of altered genes in eWAT (top), gastrocnemius muscle (bottom), and liver (boxed inset in the top) on chow and HFD. The data represent log2 ratios to a virtual pool of high-fat-fed Pro/Pro groups for each tissue. White and black bars to the right of each cluster indicate the location of Pro/Pro and Ala/Ala samples within the clusters, respectively.

(B) Cocorrelations for expressed genes against plasma adiponectin (*y* axis) and *Pparg2* gene expression (*x* axis) in eWAT (top) and gastrocnemius muscle (bottom) on chow and HFD. Each dot in the graphs represents Pearson R^2 values for the two parameters. Intensity of the color (blue, Pro/Pro; red, Ala/Ala) corresponds to the number of genes with similar cocorrelations.

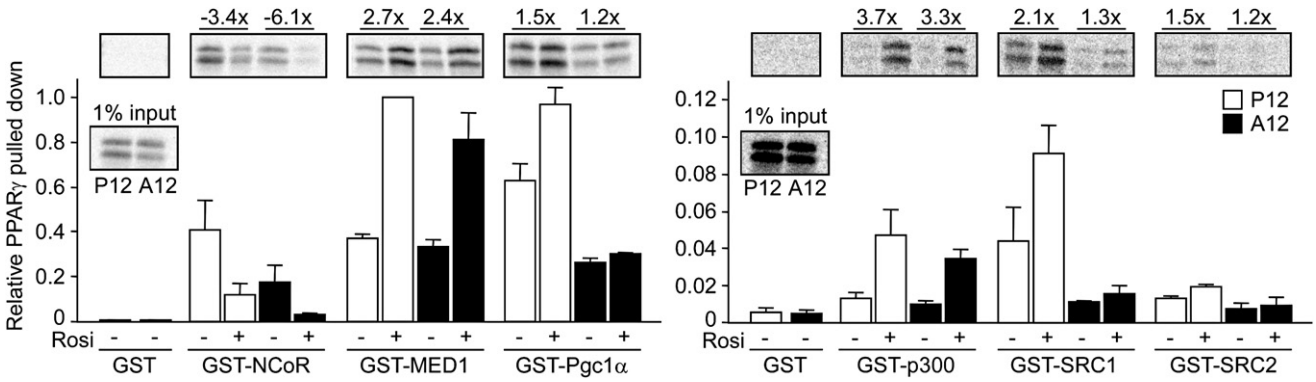

Figure 7. The Impact of the Pparγ2 Pro12Ala Variant on Cofactor Recruitment In Vitro

The effect of the Pro12Ala variant of *Pparg2* on cofactor recruitment by in vitro GST pull-down assay for select Pparγ cofactors using Pro12 or Ala12 PPARγ2 variants. Data are presented as the relative amount of PPARγ2 pulled down by the indicated cofactors in the absence (–) or presence (+) of synthetic PPARγ ligand Rosi from three independent experiments. Cofactors interacting strongly with PPARγ2 are shown on the left, with representative, short exposure blots on top displaying the fold induction of interaction upon ligand (Rosi) treatment. The cofactors with weaker interaction, requiring longer exposure, are shown on the right. The insets on the left in each panel show the corresponding exposures of 1% input. Data are presented as means ± SEM.

called TRAP220) and p300 were similar for Pro12 and Ala12 variants of PPARγ2 (Figure 7). However, the interaction of corepressor Ncor was strongly reduced with both the unliganded and liganded Ala12 mutant, although it appeared to have the capacity to release Ncor upon ligand binding similar to that of the Pro12 variant. In contrast, the basal interaction with Pgc1α and the p160 coactivator SRC-1 (and perhaps also SRC-2) was robustly decreased in the Ala12 mutant, and their ligand-dependent recruitment was totally abolished. These experiments demonstrate that the Pro12Ala mutation selectively alters the profile of coregulator recruitment. Furthermore, the ligand dependency of PPARγ2 action is also selectively altered, but in a subset of coregulators that at least partly differs from that in which interaction per se is altered.

DISCUSSION

In lean humans, the Ala12 allele of *PPARG2* has been associated with reduced risk of obesity (Altshuler et al., 2000; Deeb et al., 1998). On the other hand, Ala12 becomes the risk allele for further weight gain in obese patients (Ek et al., 1999; Masud and Ye, 2003). Correspondingly, the Ala12 allele is viewed as protective against T2DM in nonobese subjects (Altshuler et al., 2000; Deeb et al., 1998), whereas in obese subjects the effect is less clear (Ek et al., 1999). The phenotype of our Pro12Ala knockin mice essentially replicates these observations, as Ala/Ala animals were leaner and more insulin sensitive than Pro/Pro animals but had a tendency for increased weight gain and lost the benefits on insulin sensitivity upon high-fat feeding. Adipose tissue contributes to the improved insulin sensitivity of the Ala/Ala mice on chow, although a mild effect from skeletal muscle appears also likely. Indeed, it is possible that the high insulin dose (18 mU/kg/min) used in our clamp experiment had began to saturate the signaling for insulin-dependent glucose uptake, especially in the rather insulin-sensitive skeletal muscle, thus masking any small differences (Chibalin et al., 2008). Since the relative lipodystrophy of the mice deficient in Pparγ activity persists also on HFD (Jones et al., 2005; Kubota et al., 1999; Medina-Gomez et al., 2007), the increased responsiveness to HFD of Ala/Ala mice implies that in the presence of a positive energy balance, the adipogenic capacity of the Ala12 variant exceeds that of the Pro12 variant, in contrast to the apparently lower activity of the Ala12 variant on chow. Consistent with the reduced fat mass in vivo, the Ala/Ala genotype affected adipocyte maturation as well in vitro. These results collectively suggest that the Pro12Ala variant is a critical, diet-dependent metabolic sensor that, especially in the adipose tissue, modulates the efficacy of Pparγ2 in the control of gene-environment interaction. TZDs like pioglitazone, however, appear not to strongly interact with the Pro12Ala genotype upon caloric excess.

The diet-dependent impact of the Pro12Ala variant also affected circulating lipids as the improved profile in Ala/Ala mice on chow diet was obliterated on HFD. The Ala12 variant seems therefore to be beneficial to lipid homeostasis, at least when dietary fat is not in excess. Since elevated levels of triglycerides are a risk factor for the development of insulin resistance (Laakso, 2004), it is possible that in the chow-fed Pro12Ala mice, improved insulin sensitivity and lower lipid levels are causally connected.

Although the Pro12Ala variant improved lipid profiles and insulin sensitivity in lean mice, it did not affect energy metabolism at large, since RER did not differ between Pro/Pro and Ala/Ala mice on either chow or HFD. Also, thermogenesis in the high-fat-fed state was unaltered (data not shown). However, since the diet-dependent increase in the spontaneous activity of Ala/Ala mice on chow was limited to the onset of the dark period, it is intriguing to speculate whether Pro12Ala might affect behavior or some other brain-related function. Finally, the modest bone phenotype of Ala/Ala mice, reflected by an increase in bone area and mineral content in the wake of a constant mineral density, again highlighted the links between adipocytes and osteoblasts (Cock et al., 2004) and Pparγ and osteoclasts (Wan et al., 2007), which thus remain pertinent.

The increased longevity of our Pparγ2 Ala/Ala mice fully supports the earlier suggestion that humans carrying the Ala12 variant may have longer lifespans (Barbieri et al., 2004). Although the extended survival of Ala/Ala mice was not independent of

beneficial changes in fat mass, circulating lipids, and insulin sensitivity, these results nevertheless propose a role for Pparγ2 in longevity determination. Due to the high prevalence (~80%–100%) in human populations of the more active Pro12 allele, the shorter lifespan of the Pparγ2 Pro/Pro mice requires additional scrutiny in humans. Our data in fact suggest that the Ala12 isoform of Pparγ2 may functionally mimic the caloric restricted state, hence resulting in improved longevity. There results warrant also further analysis of the effects of Pparγ agonists on longevity.

From a mechanistic point of view, it is interesting to stress that the Pro12Ala mutation resides within the 30 N-terminal amino acids of the activation function 1 domain (AF1) that are unique to Pparγ2 (Fajas et al., 1997; Tontonoz et al., 1994a). This region confers the increased transcriptional capacity and adipogenic potential of Pparγ2 compared to Pparγ1 (Ren et al., 2002; Werman et al., 1997). We show here that the Pro12Ala mutation alters both ligand-dependent and ligand-independent interaction between PPARγ2 and its cofactors, like Pgc1α, SRC1, and Ncor, thus expanding the molecular basis for the Pro12Ala effects beyond decreased DNA binding efficiency (Deeb et al., 1998). Since transcriptional coregulators modulate metabolic homeostasis (Feige and Auwerx, 2007), it is likely that the selective recruitment of coregulators by the PPARγ2 Pro12Ala mutant mechanistically contributes to the metabolic phenotype of Ala/Ala mice. However, the exact contribution of the interaction with PPARγ2 versus other transcription factors to the in vivo function of individual coregulators remains elusive. Consequently, it is difficult to precisely link the results of the in vitro interaction assays with the phenotype of our mouse model.

Our gene expression results, including the consistent overexpression of *Adipor2* in Ala/Ala WAT and muscle and the modulation of cocorrelation patterns of plasma adiponectin and Pparγ2 by diet only in Ala/Ala WAT and muscle, suggest that the Ala12 mutant sensitizes the transcriptional activity of Pparγ2 in WAT and muscle to adiponectin signaling, especially when conveyed through *Adipor2*. It is thus plausible that altered adiponectin signaling contributes to the improvement of insulin sensitivity of lean Ala/Ala mice, as this adipocytokine is an insulin sensitizer (Kubota et al., 2002). Interestingly, increased adiponectin levels have been reported in Ala/Ala humans (Mousavinasab et al., 2005). The surprising finding that the expression of G protein-coupled receptors (Gpcrs) is affected by the Pro12Ala variant in WAT and liver may also have a link to adiponectin signaling, since sequence analysis has shown that adiponectin receptors are distantly related to Gpcrs (Yamauchi et al., 2003). The considerable differences in gene expression changes associating to the Pro12Ala variant between the two diets support the hypothesis that the Pro12Ala phenotype depends on nutritional status and thereby underscore that Pparγ2 functions as an environmental sensor.

Collectively, our results establish the diet-dependent influence of Pparγ2 Pro12Ala variant on metabolic control via modulated cofactor interaction and changes in gene expression patterns in mice. These data hence consolidate Pparγ2 as an important factor at the interface between genes and the environment and may provide avenues to better, possibly Pro12Ala genotype-dependent, treatment strategies for insulin resistance in T2DM and the metabolic syndrome.

EXPERIMENTAL PROCEDURES

Animal Experiments

Generation of Pparγ Pro12Ala mutant mice on a hybrid C57BL/6J/129 SV background has been described previously (Koutnikova et al., 2003). We analyzed congenic mice backcrossed onto C57Bl/6 genetic background for at least nine generations. Genotyping was performed by PCR, using standard conditions and primers HA24 (5′-GTGAATTAGCTTCCTCTC-3′) and HA26 (5′-GTGAAGCAAATCTGAATAG-3′) that produce 322 and 480 bp products from the Pro and Ala alleles, respectively. Pparγ Pro12Ala and wild-type littermates were fed regular rodent chow or HFD (D12330, 5560 kcal/kg; Research Diets; New Brunswick, NJ), as indicated. Only males were used, to minimize possible effects of variation in estrus status of females. Since the body weight development of Pro/Ala heterozygote mice was intermediate to that of Pro/Pro and Ala/Ala mice, we focused on the two homozygote genotypes in further experimentation. Mice were housed with a 12 hr light-dark cycle and had free access to water and food.

The phenotyping protocols included the following: (1) blood collection at fed or after 4 hr or overnight fast state, as indicated; (2) body composition by DEXA; (3) systolic arterial blood pressure by tail-cuff system; (4) glucose tolerance by IPGTT (16 hr fasted, 2 g glucose/kg mouse); (5) insulin sensitivity, either by euglycemic-hyperinsulinemic clamp (4 hr fast, 18 mU insulin/kg/min, clamped at 5.5 mmol/L for 60 min) or by adding to that a continuous infusion of 0.1 μCi/min D-[3-^{3}H]-glucose (Perkin Elmer) to measure basal and insulin-stimulated glucose turnover, and a 3 μCi bolus of 2-Deoxy-D-glucose-1-^{14}C (Sigma-Aldrich) to measure tissue glucose uptake; (6) cold test; and (7) 25 hr monitoring with integrated indirect calorimetry and measurements for spontaneous activity as well as food and water intake (TSE LabMaster system; Bad Homburg, Germany). These tests were performed as outlined at the EMPReSS website (http://empress.har.mrc.ac.uk) and as described (Chibalin et al., 2008; Lagouge et al., 2006). Tissue collection and clinical biochemistry was performed as described (Koutnikova et al., 2003). LDL cholesterol was calculated as the difference between total and HDL cholesterol or analyzed using a fast lipoprotein liquid chromatography method (März et al., 1993). Unless specified otherwise, n = 5–8 mice per group were used in all in vivo experiments.

Survival cohort consisted of 57 Pro/Pro and 25 Ala/Ala mice. Deaths were recorded weekly. Mice observed as moribund were euthanized and recorded as dead on that week. All Pro/Pro mice reached the endpoint, but a few Ala/Ala mice survived at the time of analysis.

Molecular Methods

RNA was isolated using the TRIzol Reagent (Invitrogen; Carslbad, CA) or RNeasy Mini or Lipid Tissue Mini kits (QIAGEN; Hilden, Germany). Synthesis of cDNA was performed using the SuperScript II System (Invitrogen) and random hexamer primers. Quantitative RT-PCR was performed by using QuantiTect SYBR Green PCR Kit from QIAGEN according to the manufacturer's protocols. As the invariant control, *18S* rRNA or peptidylprolyl isomerase B (*Ppib*, also called *Cyclophilin B*) mRNA or both was used. Primer sequences are available at http://www-igbmc.u-strasbg.fr/recherche/Dep_NG/Eq_JAuwe/Publi/Paper.html.

Nuclear protein extraction, immunoprecipitation, and immunoblotting were performed as described (Lagouge et al., 2006), using Pparγ antibodies from Santa Cruz.

GST pull-down experiments were performed as described (Feige et al., 2007). The coregulator interacting domains fused to GST were expressed in *E. coli* from plasmids as described (Feige et al., 2007; Rocchi et al., 2001) and purified on a glutathione affinity matrix (Pharmacia). Human PPARγ2 Pro12 and Ala12 isoforms were produced in reticulocyte lysates (Promega) in the presence of ^{35}S-Methionine, and the amounts of receptor were equalized to normalize for differences in production efficiency.

Adipocyte Differentiation

MEFs from Pparγ2 Pro/Pro and Ala/Ala embryos were differentiated to adipocytes and further analyzed as described (Fajas et al., 2002).

Gene Expression Profiling

Eight-week-old male Pro/Pro and Ala/Ala littermate mice were fed either regular rodent chow or HFD (as above) for 15 weeks (n = 8–10 per group), at which

time blood and tissue samples were collected. Total RNA extraction, sample amplification, labeling, and microarray (Genechip Mouse Genome 430 2.0 Array; Affymetrix, Inc.; Santa Clara, CA) processing steps were performed by the Rosetta Inpharmatics Gene Expression Laboratory (Seattle, WA) using custom automated procedures, in compliance with manufacturer protocols.

Data Analysis

For computation of the statistics from the mouse data, SPSS version 14 for Windows (Chicago, IL) was used. Data are presented as means ± SEM. None of the variables significantly deviated from normal distribution (One-Sample Kolmogorov-Smirnov Test). Two-tailed Student's t test was used for comparing means. Survival was tested using Kaplan-Meier statistics. Full factorial univariate linear modeling was used to analyze the effect of several factors. For correlation analysis, Pearson correlation was used. Microarray data were processed using Rosetta Resolver (Rosetta Inpharmatics; Seattle, WA) and expressed as relative to the virtual pool of Pro/Pro mice fed with an HFD (mlratio). Gene expression signatures were generated from these mlratios for expressed genes (25% of RMA processed intensities above 60% quantile) by t testing (Pro/Pro versus Ala/Ala) and correcting for multiple testing (20% cutoff for False Discovery Rate). GSEA was performed according to provider suggestions, Pro/Pro versus Ala/Ala. Statistical significance was declared if $p < 0.05$.

ACCESSION NUMBERS

The NCBI GEO Series accession number for the microarray data reported in this paper is GSE13305.

SUPPLEMENTAL DATA

Supplemental Data include three figures and four tables and can be found online at http://www.cell.com/cellmetabolism/supplemental/S1550-4131(08)00359-8.

ACKNOWLEDGMENTS

We acknowledge grant support of the NIH (DK067320-01), the European Union (Eugene2; LSHM-CT-2004-512013), CNRS, INSERM, ULP, the Hôpital Universitaire de Strasbourg, EPFL, Merck Research Laboratories, and the Academy of Finland (grant number 124243). We thank the members of the Auwerx Laboratory and Doctors Thomas Vogt, Nancy Thornberry, and Michael Coon for helpful discussions and support.

Received: February 19, 2008
Revised: September 1, 2008
Accepted: November 14, 2008
Published: January 6, 2009

REFERENCES

Altshuler, D., Hirschhorn, J.N., Klannemark, M., Lindgren, C.M., Vohl, M.C., Nemesh, J., Lane, C.R., Schaffner, S.F., Bolk, S., Brewer, C., et al. (2000). The common PPARgamma Pro12Ala polymorphism is associated with decreased risk of type 2 diabetes. Nat. Genet. *26*, 76–80.

Auwerx, J. (1999). PPARgamma, the ultimate thrifty gene. Diabetologia *42*, 1033–1049.

Barbieri, M., Bonafe, M., Rizzo, M.R., Ragno, E., Olivieri, F., Marchegiani, F., Franceschi, C., and Paolisso, G. (2004). Gender specific association of genetic variation in peroxisome proliferator-activated receptor (PPAR)gamma-2 with longevity. Exp. Gerontol. *39*, 1095–1100.

Bordone, L., and Guarente, L. (2005). Calorie restriction, SIRT1 and metabolism: understanding longevity. Nat. Rev. Mol. Cell Biol. *6*, 298–305.

Chibalin, A.V., Leng, Y., Vieira, E., Krook, A., Bjornholm, M., Long, Y.C., Kotova, O., Zhong, Z., Sakane, F., Steiler, T., et al. (2008). Downregulation of diacylglycerol kinase delta contributes to hyperglycemia-induced insulin resistance. Cell *132*, 375–386.

Cock, T.A., Back, J., Elefteriou, F., Karsenty, G., Kastner, P., Chan, S., and Auwerx, J. (2004). Enhanced bone formation in lipodystrophic PPARgamma (hyp/hyp) mice relocates haematopoiesis to the spleen. EMBO Rep. *5*, 1007–1012.

Deeb, S.S., Fajas, L., Nemoto, M., Pihlajamäki, J., Mykkänen, L., Kuusisto, J., Laakso, M., Fujimoto, W., and Auwerx, J. (1998). A Pro12Ala substitution in PPARgamma2 associated with decreased receptor activity, lower body mass index and improved insulin sensitivity. Nat. Genet. *20*, 284–287.

Ek, J., Urhammer, S.A., Sorensen, T.I., Andersen, T., Auwerx, J., and Pedersen, O. (1999). Homozygosity of the Pro12Ala variant of the peroxisome proliferation-activated receptor-gamma2 (PPAR-gamma2): divergent modulating effects on body mass index in obese and lean Caucasian men. Diabetologia *42*, 892–895.

Fajas, L., Auboeuf, D., Raspe, E., Schoonjans, K., Lefebvre, A.M., Saladin, R., Najib, J., Laville, M., Fruchart, J.C., Deeb, S., et al. (1997). The organization, promoter analysis, and expression of the human PPARgamma gene. J. Biol. Chem. *272*, 18779–18789.

Fajas, L., Egler, V., Reiter, R., Hansen, J., Kristiansen, K., Debril, M.B., Miard, S., and Auwerx, J. (2002). The retinoblastoma-histone deacetylase 3 complex inhibits PPARgamma and adipocyte differentiation. Dev. Cell *3*, 903–910.

Feige, J.N., and Auwerx, J. (2007). Transcriptional coregulators in the control of energy homeostasis. Trends Cell Biol. *17*, 292–301.

Feige, J.N., Gelman, L., Rossi, D., Zoete, V., Metivier, R., Tudor, C., Anghel, S.I., Grosdidier, A., Lathion, C., Engelborghs, Y., et al. (2007). The endocrine disruptor monoethyl-hexyl-phthalate is a selective peroxisome proliferator-activated receptor gamma modulator that promotes adipogenesis. J. Biol. Chem. *282*, 19152–19166.

Florez, J.C., Hirschhorn, J., and Altshuler, D. (2003). The inherited basis of diabetes mellitus: implications for the genetic analysis of complex traits. Annu. Rev. Genomics Hum. Genet. *4*, 257–291.

Heikkinen, S., Auwerx, J., and Argmann, C.A. (2007). PPARgamma in human and mouse physiology. Biochim. Biophys. Acta *1771*, 999–1013.

Hotta, K., Gustafson, T.A., Yoshioka, S., Ortmeyer, H.K., Bodkin, N.L., and Hansen, B.C. (1998). Relationships of PPARgamma and PPARgamma2 mRNA levels to obesity, diabetes and hyperinsulinaemia in rhesus monkeys. Int. J. Obes. Relat. Metab. Disord. *22*, 1000–1010.

Jones, J.R., Barrick, C., Kim, K.A., Lindner, J., Blondeau, B., Fujimoto, Y., Shiota, M., Kesterson, R.A., Kahn, B.B., and Magnuson, M.A. (2005). Deletion of PPARgamma in adipose tissues of mice protects against high fat diet-induced obesity and insulin resistance. Proc. Natl. Acad. Sci. USA *102*, 6207–6212.

Knouff, C., and Auwerx, J. (2004). Peroxisome proliferator-activated receptor-gamma calls for activation in moderation: lessons from genetics and pharmacology. Endocr. Rev. *25*, 899–918.

Koutnikova, H., Cock, T.A., Watanabe, M., Houten, S.M., Champy, M.F., Dierich, A., and Auwerx, J. (2003). Compensation by the muscle limits the metabolic consequences of lipodystrophy in PPAR gamma hypomorphic mice. Proc. Natl. Acad. Sci. USA *100*, 14457–14462.

Kubota, N., Terauchi, Y., Miki, H., Tamemoto, H., Yamauchi, T., Komeda, K., Satoh, S., Nakano, R., Ishii, C., Sugiyama, T., et al. (1999). PPAR gamma mediates high-fat diet-induced adipocyte hypertrophy and insulin resistance. Mol. Cell *4*, 597–609.

Kubota, N., Terauchi, Y., Yamauchi, T., Kubota, T., Moroi, M., Matsui, J., Eto, K., Yamashita, T., Kamon, J., Satoh, H., et al. (2002). Disruption of adiponectin causes insulin resistance and neointimal formation. J. Biol. Chem. *277*, 25863–25866.

Laakso, M. (2004). Gene variants, insulin resistance, and dyslipidaemia. Curr. Opin. Lipidol. *15*, 115–120.

Lagouge, M., Argmann, C., Gerhart-Hines, Z., Meziane, H., Lerin, C., Daussin, F., Messadeq, N., Milne, J., Lambert, P., Elliott, P., et al. (2006). Resveratrol improves mitochondrial function and protects against metabolic disease by activating SIRT1 and PGC-1alpha. Cell *127*, 1109–1122.

Lehmann, J.M., Moore, L.B., Smith-Oliver, T.A., Wilkison, W.O., Willson, T.M., and Kliewer, S.A. (1995). An antidiabetic thiazolidinedione is a high affinity

ligand for peroxisome proliferator-activated receptor gamma (PPAR gamma). J. Biol. Chem. *270*, 12953–12956.

Lehrke, M., and Lazar, M.A. (2005). The many faces of PPARgamma. Cell *123*, 993–999.

Luan, J., Browne, P.O., Harding, A.H., Halsall, D.J., O'Rahilly, S., Chatterjee, V.K., and Wareham, N.J. (2001). Evidence for gene-nutrient interaction at the PPARgamma locus. Diabetes *50*, 686–689.

Ludovico, O., Pellegrini, F., Di Paola, R., Minenna, A., Mastroianno, S., Cardellini, M., Marini, M.A., Andreozzi, F., Vaccaro, O., Sesti, G., and Trischitta, V. (2007). Heterogeneous effect of peroxisome proliferator-activated receptor gamma2 Ala12 variant on type 2 diabetes risk. Obesity (Silver Spring) *15*, 1076–1081.

Masud, S., and Ye, S. (2003). Effect of the peroxisome proliferator activated receptor-gamma gene Pro12Ala variant on body mass index: a meta-analysis. J. Med. Genet. *40*, 773–780.

Masugi, J., Tamori, Y., Mori, H., Koike, T., and Kasuga, M. (2000). Inhibitory effect of a proline-to-alanine substitution at codon 12 of peroxisome proliferator-activated receptor-gamma 2 on thiazolidinedione-induced adipogenesis. Biochem. Biophys. Res. Commun. *268*, 178–182.

Medina-Gomez, G., Gray, S.L., Yetukuri, L., Shimomura, K., Virtue, S., Campbell, M., Curtis, R.K., Jimenez-Linan, M., Blount, M., Yeo, G.S., et al. (2007). PPAR gamma 2 prevents lipotoxicity by controlling adipose tissue expandability and peripheral lipid metabolism. PLoS Genet. *3*, e64.

Memisoglu, A., Hu, F.B., Hankinson, S.E., Manson, J.E., De Vivo, I., Willett, W.C., and Hunter, D.J. (2003). Interaction between a peroxisome proliferator-activated receptor gamma gene polymorphism and dietary fat intake in relation to body mass. Hum. Mol. Genet. *12*, 2923–2929.

Mootha, V.K., Lindgren, C.M., Eriksson, K.F., Subramanian, A., Sihag, S., Lehar, J., Puigserver, P., Carlsson, E., Ridderstrale, M., Laurila, E., et al. (2003). PGC-1alpha-responsive genes involved in oxidative phosphorylation are coordinately downregulated in human diabetes. Nat. Genet. *34*, 267–273.

Mousavinasab, F., Tähtinen, T., Jokelainen, J., Koskela, P., Vanhala, M., Oikarinen, J., Keinänen-Kiukaanniemi, S., and Laakso, M. (2005). Common polymorphisms in the PPARgamma2 and IRS-1 genes and their interaction influence serum adiponectin concentration in young Finnish men. Mol. Genet. Metab. *84*, 344–348.

März, W., Siekmeier, R., Scharnagl, H., Seiffert, U.B., and Gross, W. (1993). Fast lipoprotein chromatography: new method of analysis for plasma lipoproteins. Clin. Chem. *39*, 2276–2281.

Ren, D., Collingwood, T.N., Rebar, E.J., Wolffe, A.P., and Camp, H.S. (2002). PPARgamma knockdown by engineered transcription factors: exogenous PPARgamma2 but not PPARgamma1 reactivates adipogenesis. Genes Dev. *16*, 27–32.

Rocchi, S., Picard, F., Vamecq, J., Gelman, L., Potier, N., Zeyer, D., Dubuquoy, L., Bac, P., Champy, M.F., Plunket, K.D., et al. (2001). A unique PPARgamma ligand with potent insulin-sensitizing yet weak adipogenic activity. Mol. Cell *8*, 737–747.

Saxena, R., Voight, B.F., Lyssenko, V., Burtt, N.P., de Bakker, P.I., Chen, H., Roix, J.J., Kathiresan, S., Hirschhorn, J.N., Daly, M.J., et al. (2007). Genome-wide association analysis identifies loci for type 2 diabetes and triglyceride levels. Science *316*, 1331–1336.

Scott, L.J., Mohlke, K.L., Bonnycastle, L.L., Willer, C.J., Li, Y., Duren, W.L., Erdos, M.R., Stringham, H.M., Chines, P.S., Jackson, A.U., et al. (2007). A genome-wide association study of type 2 diabetes in Finns detects multiple susceptibility variants. Science *316*, 1341–1345.

Sladek, R., Rocheleau, G., Rung, J., Dina, C., Shen, L., Serre, D., Boutin, P., Vincent, D., Belisle, A., Hadjadj, S., et al. (2007). A genome-wide association study identifies novel risk loci for type 2 diabetes. Nature *445*, 881–885.

Steinthorsdottir, V., Thorleifsson, G., Reynisdottir, I., Benediktsson, R., Jonsdottir, T., Walters, G.B., Styrkarsdottir, U., Gretarsdottir, S., Emilsson, V., Ghosh, S., et al. (2007). A variant in CDKAL1 influences insulin response and risk of type 2 diabetes. Nat. Genet. *39*, 770–775.

Subramanian, A., Tamayo, P., Mootha, V.K., Mukherjee, S., Ebert, B.L., Gillette, M.A., Paulovich, A., Pomeroy, S.L., Golub, T.R., Lander, E.S., and Mesirov, J.P. (2005). Gene set enrichment analysis: a knowledge-based approach for interpreting genome-wide expression profiles. Proc. Natl. Acad. Sci. USA *102*, 15545–15550.

Tontonoz, P., Hu, E., Graves, R.A., Budavari, A.I., and Spiegelman, B.M. (1994a). mPPAR gamma 2: tissue-specific regulator of an adipocyte enhancer. Genes Dev. *8*, 1224–1234.

Tontonoz, P., Hu, E., and Spiegelman, B.M. (1994b). Stimulation of adipogenesis in fibroblasts by PPAR gamma 2, a lipid-activated transcription factor. Cell *79*, 1147–1156.

Tönjes, A., Scholz, M., Loeffler, M., and Stumvoll, M. (2006). Association of Pro12Ala polymorphism in peroxisome proliferator-activated receptor {gamma} with pre-diabetic phenotypes: meta-analysis of 57 studies on nondiabetic individuals. Diabetes Care *29*, 2489–2497.

Vidal-Puig, A.J., Considine, R.V., Jimenez-Linan, M., Werman, A., Pories, W.J., Caro, J.F., and Flier, J.S. (1997). Peroxisome proliferator-activated receptor gene expression in human tissues. Effects of obesity, weight loss, and regulation by insulin and glucocorticoids. J. Clin. Invest. *99*, 2416–2422.

Wan, Y., Chong, L.W., and Evans, R.M. (2007). PPAR-gamma regulates osteoclastogenesis in mice. Nat. Med. *13*, 1496–1503.

Werman, A., Hollenberg, A., Solanes, G., Bjorbaek, C., Vidal-Puig, A.J., and Flier, J.S. (1997). Ligand-independent activation domain in the N terminus of peroxisome proliferator-activated receptor gamma (PPARgamma). Differential activity of PPARgamma1 and −2 isoforms and influence of insulin. J. Biol. Chem. *272*, 20230–20235.

Yamauchi, T., Kamon, J., Ito, Y., Tsuchida, A., Yokomizo, T., Kita, S., Sugiyama, T., Miyagishi, M., Hara, K., Tsunoda, M., et al. (2003). Cloning of adiponectin receptors that mediate antidiabetic metabolic effects. Nature *423*, 762–769.

Zeggini, E., Weedon, M.N., Lindgren, C.M., Frayling, T.M., Elliott, K.S., Lango, H., Timpson, N.J., Perry, J.R., Rayner, N.W., Freathy, R.M., et al. (2007). Replication of genome-wide association signals in UK samples reveals risk loci for type 2 diabetes. Science *316*, 1336–1341.